

# Overexpression of Mig-6 in Cartilage Induces an Osteoarthritis-Like Phenotype in Mice

**Melina Bellini**

Western University

**Michael Andrew Pest**

Western University

**Manuela Miranda Rodrigues**

Western University

**Ling Qin**

University of Pennsylvania Perelman School of Medicine

**Jae-Wook Jeong**

Michigan State University

**Frank Beier** (✉ [fbeier@uwo.ca](mailto:fbeier@uwo.ca))

Western University <https://orcid.org/0000-0002-4619-6964>

---

## Research article

**Keywords:** Mitogen inducible gene-6, Epidermal growth factor receptor, Osteoarthritis, Articular cartilage

**Posted Date:** April 29th, 2020

**DOI:** <https://doi.org/10.21203/rs.2.24144/v2>

**License:**  This work is licensed under a Creative Commons Attribution 4.0 International License.

[Read Full License](#)

---

**Version of Record:** A version of this preprint was published at Arthritis Research & Therapy on May 19th, 2020. See the published version at <https://doi.org/10.1186/s13075-020-02213-z>.

# Abstract

**Background:** Osteoarthritis (OA) is the most common form of arthritis and characterized by degeneration of articular cartilage. Mitogen-inducible gene 6 (Mig-6) has been identified as a negative regulator of the Epidermal Growth Factor Receptor (EGFR). Cartilage-specific *Mig-6* knockout (KO) mice display increased EGFR signaling, an anabolic buildup of articular cartilage and formation of chondro-osseous nodules. Since our understanding of the EGFR/Mig-6 network in cartilage remains incomplete, we characterized mice with cartilage-specific overexpression of Mig-6 in this study.

**Methods:** Utilizing knee joints from cartilage-specific *Mig-6* overexpressing (*Mig-6<sup>over/over</sup>*) mice (at multiple time points), we evaluated the articular cartilage using histology, immunohistochemical staining and semi-quantitative histopathological scoring (OARSI) at multiple ages. MicroCT analysis was employed to examine skeletal morphometry, body composition, and bone mineral density.

**Results:** Our data show that cartilage-specific *Mig-6* overexpression did not cause any major developmental abnormalities in articular cartilage, although *Mig-6<sup>over/over</sup>* mice have slightly shorter long bones compared to the control group. Moreover, there was no significant difference in bone mineral density and body composition in any of the groups. However, our results indicate that *Mig-6<sup>over/over</sup>* male mice show accelerated cartilage degeneration at 12 and 18 months of age. Immunohistochemistry for SOX9 demonstrated that the number of positively stained cells in *Mig-6<sup>over/over</sup>* mice was decreased relative to controls. Immunostaining for MMP13 appeared increased in areas of cartilage degeneration in *Mig-6<sup>over/over</sup>* mice. Moreover, staining for phospho-EGFR (Tyr-1173) and lubricin (PRG4) was decreased in the articular cartilage of *Mig-6<sup>over/over</sup>* mice. **Conclusion:** Overexpression of *Mig-6* in articular cartilage causes no major developmental phenotype; however, these mice develop earlier OA during aging. These data demonstrate that Mig-6/EGFR pathways is critical for joint homeostasis and might present a promising therapeutic target for OA.

## Introduction

Osteoarthritis (OA), a chronic degenerative joint disease, is the most common form of arthritis. OA affects 242 million individuals worldwide, but that number will grow due to increasing life expectancies (1). This statistic is alarming, considering the disability, the loss of quality of life, and the costs to the health system generated by OA. Currently, there are pharmacological treatments available to manage OA symptoms such as pain (2–4) as well as surgical joint replacement at the end stage of disease (5,6). Unfortunately however, there is no cure for OA. Progressive understanding of the pathophysiology of OA suggests that the disease is a heterogeneous condition, so further research is needed to direct the clinical approaches to disease management (7).

Recent studies have shown that OA is a multifactorial disease of the whole joint, however its pathogenesis remains still poorly understood (8). Genetic, environmental, and biomechanical factors can accelerate the onset of OA (9). Articular cartilage is a highly specialized tissue that forms the smooth

gliding surface of synovial joints, with chondrocytes as the only cellular component of cartilage (10). The homeostasis of the cartilage extracellular matrix (ECM) involves a dynamic equilibrium between anabolic and catabolic pathways controlled by chondrocytes (11). The progression of OA is associated with dramatic alteration in the integrity of the cartilage ECM network formed by a large number of proteoglycans (mostly aggrecan), collagen II, and other non-collagenous matrix proteins (12). In addition, ECM synthesis is regulated by a number of transcriptional regulators involved in chondrogenesis, specifically Sex-determining-region-Y Box 9 (SOX9), L-SOX 5 and SOX6 that regulate type II collagen (*Col2a1*) and Aggrecan (*Acan*) gene expression (13). On the other hand, catabolic events are dominant in OA and cells are exposed to degenerative enzymes such as aggrecanases (e.g. ADAMTS-4, -5) (12,14), collagenases (e.g. MMP-1,-3, -8, -13) (15), and gelatinases (e.g. MMP-2, and MMP-9), all of which have implications in articular cartilage degeneration (16). A number of growth factors (17) play a role in OA pathology, such as transforming growth factor- $\beta$  (18), BMP-2 (19), Insulin growth factor 1 (IGF-1) (20) fibroblast growth factor (FGF) and others, but the exact regulation of chondrocyte physiology is still not completely understood.

Recent studies in our laboratory (21,22) have identified the epidermal growth factor receptor (EGFR) and its ligand transforming growth factor alpha (TGF $\alpha$ ) as possible mediators of cartilage degeneration (23–25). The human *TGFA* gene locus was also strongly linked to hip OA and cartilage thickness in genome-wide association studies (26,27). TGF $\alpha$  stimulates EGFR signaling and activates various cell-signaling pathways in chondrocytes, including extracellular signal-regulated kinase 1 and 2 (ERK1/2) and phosphoinositide 3-kinase (P13K) (28). EGFR signaling plays important roles in endochondral ossification (29,30), growth plate development (29) and cartilage maintenance and homeostasis (31–33), but many aspects of its action in cartilage are still not well understood. However, both protective and catabolic effects of EGFR signaling in OA have been reported, suggesting context-specific roles of this pathway (34).

Mitogen-inducible gene 6 (Mig-6) is also known as Gene 33, ErbB receptor feedback inhibitor 1 (ERRFI1), or RALT, and is found in the cytosol (35). *Mig-6* protein binds to and inhibits EGFR signaling through a two-tiered mechanism: suppression of EGFR catalytic activity and receptor down-regulation (36). Interestingly, various studies have reported that loss of Mig-6 induces the onset of OA-like symptoms in mice (35,37–39). Cartilage-specific (Col2-Cre) knockout of *Mig-6* mice results in formation of chondro-osseous nodules in the knee, but also increased thickness of articular cartilage in the knee, ankle, and elbow (40). *Prx1*-Cre-mediated knockout of *Mig-6* in the limb mesenchyme results in a similar phenotype as that observed in cartilage-specific knockout mice (32). These phenotypes appeared to be caused by an increase in chondrocyte proliferation in articular cartilage, supported by increased expression of Sox9 and EGFR activation in cartilage (32). Since our studies suggest dosage- and/or context-specific roles of EGFR signaling in the process of cartilage degeneration in OA, in this study we used a cartilage-specific (Col2-Cre) to examine effects of Mig-6 overexpression specifically in articular cartilage. We hypothesized that overexpression of Mig-6/EGFR accelerates cartilage degeneration during aging.

# Materials And Methods

## Generation of Mig-6 overexpression mice

*Mig-6* overexpression animals on a mixed C57Bl/6 and agouti mouse background, with the overexpression cassette in the Rosa26 locus (41) and bred for 10 generations into a C57Bl/6 background. Transcription of *Mig-6* is under the control of a ubiquitously expressed chicken beta actin-cytomegalovirus hybrid (CAGGS) promoter, but blocked by a “Stop Cassette” flanked by LoxP sites (LSL) (41). *Mig-6* overexpression mice were bred to mice carrying the Cre recombinase gene under the control of the Collagen 2 promoter (42), to induce recombination and removal of the Stop Cassette specifically in cartilage. Throughout the manuscript, animals for homozygote overexpression of Mig-6 from both alleles are termed *Mig-6<sup>over/over</sup>* (*Mig-6<sup>over/over</sup>Col2a1-Cre<sup>+/-</sup>*), while control mice are identical but without the Cre gene (noted as “control” in this manuscript for simplicity). Mice were group housed (at least one pair of littermate matched control and overexpression animals), on a standard 12-hour light/dark cycle, without access to running wheels, and with free access to mouse chow and water. Animals were weighed prior to euthanasia by asphyxiation with CO<sub>2</sub>. All animal experiments were done in accordance with the Animal Use Subcommittee at the University of Western Ontario and conducted in accordance with guidelines from the Canadian Council on Animal Care.

## Genotyping

Genotype was determined by polymerase chain reaction (PCR) analysis using DNA processed from biopsy samples of ear tissue from mice surviving to at least 21 days of age. PCR strategy: Primer set P1 and P2 can amplify a 300 bp fragment from the wild-type allele, whereas P1 and P3 can amplify a 450 bp fragment from the targeted ROSA26 locus allele (41) (Supplementary Figure/Table 1).

## RNA isolation and quantitative real-time PCR

Total RNA was isolated from post-natal day 0 (P0) mouse cartilage of *Mig-6<sup>over/over</sup>* and control littermates using TRIzol® (Invitrogen) as per manufacturer’s instructions and as previously described (43). Complementary DNA (cDNA) was synthesized using the iScript cDNA Synthesis kit (Bio-Rad) with 1 µg of RNA (Bio-Rad Laboratories), and combined with 300nM of forward and reverse primers (for primer sequences, please see Supplementary Figure 1E) as well as iQ™ SYBR® Green Supermix (Bio-Rad Laboratories) for PCR on a Bio-Rad CFX384 RT-PCR system. Relative gene expression was normalized to the internal control Glyceraldehyde 3-phosphate dehydrogenase (*Gapdh*), calculated using the  $\Delta\Delta CT$  method.

**Histopathology of the knee** Limbs from *Mig-6<sup>over/over</sup>* and control mice were harvested and fixed in 4% paraformaldehyde (Sigma) for 24 hours and decalcified in ethylenediaminetetraacetic acid (5% EDTA in phosphate buffered saline (PBS), pH 7.0. Joints were processed and embedded in paraffin in sagittal or frontal orientation, with serial sections taken at a thickness of 5 µm. Sections were stained with Toluidine

Blue (0.04% toluidine blue in 0.2M acetate buffer, pH 4.0, for 10 minutes) for glycosaminoglycan content and general evaluation of articular cartilage. All images were taken with a Leica DFC295 digital camera and a Leica DM1000 microscope.

**Thickness of proximal tibia growth plate** For early developmental time points such as newborn (P0), sagittal knee sections stained with toluidine blue were used to measure the width of the zones of the epiphyseal growth plate in the proximal tibia. The average thickness of the resting and proliferative zones combined was evaluated by taking three separate measurements at approximately equal intervals across the width of the growth plate. The average hypertrophic zone thickness was also measured using 3 different measurements across the width of the growth plate, starting each measurement at the border of the proliferative and hypertrophic zones and ending at the subchondral bone interface. A third average measurement was then taken of the thickness of the entire growth plate. ImageJ Software (v.1.51) (44) was used for all measures, with the observer blinded to the genotype.

**Articular cartilage evaluation** Articular cartilage thickness was measured from toluidine blue-stained frontal sections by a blinded observer. Articular cartilage thickness was measured separately for the non-calcified articular cartilage (measured from the superficial tangential zone to the tidemark) and the calcified articular cartilage (measured from the subchondral bone to the tidemark) across three evenly spaced points from all four quadrant of the joint (medial/lateral tibia and femur) in 4 sections spanning at least 500  $\mu\text{m}$ . ImageJ Software (v.1.51) (44) was used to measure the thickness of articular cartilage.

**Micro-Computerized Tomography ( $\mu\text{CT}$ )** Whole body scans were collected in 6 week-, 11 week-, 12 month- and 18 month-old control and *Mig-6<sup>over/over</sup>* male and female mice. Mice were euthanized and imaged using General Electric (GE) SpeCZT microCT machine (45) at a resolution of 50 $\mu\text{m}$ /voxel or 100 $\mu\text{m}$ /voxel. GE Healthcare MicroView software (v2.2) was used to generate 2D maximum intensity projection and 3D isosurface images to evaluate skeletal morphology. MicroView was used to create a line measurement tool in order to calculate the bone lengths, femurs lengths were calculated from the proximal point of the greater trochanter to the base of the lateral femoral condyle. Tibiae lengths were measured from the midpoint medial plateau to the medial malleolus. Humerus lengths were measured from the midpoint of the greater tubercle to the center of the olecranon fossa.

**Body composition analysis** MicroView software (GE Healthcare Biosciences) was used to analyse the microCT scans at the resolution of 100 $\mu\text{m}$ /voxel. Briefly, the region of interest (ROI) was used to calculate the mean of air, water and an epoxy-based, cortical bone-mimicking calibrator (SB3; Gammex, Middleton, WI, USA) (1100 $\text{mg}/\text{cm}^3$ ) (46). A different set of global thresholds was applied to measure adipose, lean and skeletal mass (- 275, - 40 and 280 Hounsfield Units (HU), respectively). Moreover, bone mineral density (BMD) was acquired as the ratio of the average HU (from the value of skeletal region of interest ) in order to calculate HU value of the SB3 calibrator, multiplied by the known density of the SB3 as described (45).

## OARSI histopathology scoring

Serial sections through the entire knee joint were scored according to the OARSI histopathology scoring system (47) by two blinded observers on the four quadrants of the knee: lateral femoral condyle (LFC), lateral tibial plateau (LTP), medial femoral condyle (MFC), and medial tibial plateau (MTP). Histologic scoring from 0-6 represent the OA severity, from 0 (healthy cartilage) to 6 (erosion of more than 75% of articular cartilage). Individual scores are averaged first for each observer, then across observers, and OA severity is shown as described for each graph. Scores were compared between male and female *Mig-6<sup>over/over</sup>* and control mice at both 12 and 18 months of age. All images were taken with a Leica DFC295 digital camera and a Leica DM1000 microscope.

## Immunohistochemistry

Frontal paraffin sections of knees were used to for immunohistochemical analysis, with slides with 'no primary antibody' as control. All sections were deparaffinized and rehydrated as previously described (40,48). Subsequently, the sections were incubated in 3% H<sub>2</sub>O<sub>2</sub> in methanol for 15 minutes to inhibit endogenous peroxidase activity. After rising with water, 5% goat or donkey serum in PBS was applied to reduce nonspecific background staining. Sections were incubated overnight at 4°C with primary antibodies against SOX9 (R&D Systems, AF3075), MMP13 (Protein Tech, Chicago, IL, USA, 18165-1-AP), lubricin (Abcam, ab28484) ) (primary concentration antibody for all three 1:100) and phospho-EGFR (phosphoTyr-1173; Cell Signaling Technology) (primary concentration antibody 1:50). After washing, sections were incubated with horseradish peroxidase (HRP)-conjugated donkey anti-goat or goat anti-rabbit secondary antibody (R&D system and Santa Cruz, secondary concentration antibody 1:200), before incubation with diaminobenzidine substrate as a chromogen (Dako, Canada). Finally, sections were counterstained with 0.5% methyl green (Sigma) and mounted. Cell density of articular cartilage chondrocytes from 6 and 11 weeks-old male mice was determined by counting all lacunae with evidence of nuclear staining in the lateral and medial femur/tibia using a centered region of interest measuring 200 µm wide and 70 µm deep from the articular surface by a blinded observer. For newborn (P0) animals the region of interest measured 200 µm wide and 100 µm deep from the proliferative zone.

## Statistical analysis

All statistical analyses were performed using GraphPad Prism (v6.0). Differences between two groups were evaluated using Student's *t*-test, and Two-Way ANOVA was used to compare 4 groups followed by a Bonferroni multiple comparisons test. All *n* values represent the number of cartilage specific *Mig-6* overexpressing mice and control littermates used in each group.

## Results

### Increased MIG-6 mRNA from overexpression of *Mig-6* mice and decreased EGFR staining

We bred mice for conditional overexpression of Mig-6 (41) to mice expressing Cre recombinase under control of the collagen II promoter. Homozygote mice overexpressed Mig-6 in all collagen II-producing cells (and their progeny) from both Rosa26 alleles and are referred to as *Mig-6<sup>over/over</sup>* from here on. Control mice do not express Cre. Genomic DNA was extracted from ear notches to identify homozygous mice *Mig-6<sup>over/over</sup>* using standard PCR analysis. Overexpressing mice were obtained at the expected Mendelian ratios (data not shown). Real-time RT-PCR revealed increased levels of *Mig-6* expression in cartilage of *Mig-6<sup>over/over</sup>* mice from post-natal day 0 (P0) (Figure 1A). Since Mig-6 *negatively regulates EGFR* signaling (31,32,40), immunohistochemistry was performed for phospho-EGFR (Tyr-1173) (pEGFR), with no primary antibody controls. Frontal knee sections from 11 weeks-old male *Mig-6<sup>over/over</sup>* mice showed decreased pEGFR staining in the medial compartment in the knee joint (Fig. 1B-E), as expected upon Mig-6 overexpression.

### **Overexpression of Mig-6 has minor effects on skeletal phenotypes during development**

Male mutant gained weight at the same rate as controls over the examined 10-week period, while female *Mig-6<sup>over/over</sup>* mice were slightly lighter than controls starting at 8 weeks of age (Suppl. Fig. 2A-B). These differences persisted at 12 months of age for female mice, while at 18 months both male and female mutant mice were lighter than their controls (Suppl. Fig. 2C-D). Growth plates of post-natal day 0 (P0) *Mig-6<sup>over/over</sup>* and control mice were analyzed by histology. No major differences in tibia growth plate architecture were seen between genotypes (Suppl. Fig. 3A). While the length of the total growth plate was slightly reduced in *Mig-6<sup>over/over</sup>* mice, differences in lengths of either the combined resting/proliferative or hypertrophic zones were not statistically significant (Suppl. Fig. 3B-D).

### **Mice overexpressing Mig-6 have shorter long bones than control mice**

Skeletal morphology and bone length were examined by microCT mice at the ages of 6 and weeks, and 12 and 18 months. Scans of *Mig-6<sup>over/over</sup>* male and female mice and their controls were used to generate 3D isosurface reconstructions of 100µm/voxel uCT scans, in order to measure long bones lengths (femurs, humeri, and tibiae) in GE MicroView v2.2 software. Mutant bones were slightly shorter throughout life, with the exception of the male humeri at 12 months that did not show any statistically significant difference (Fig. 2A-D). In contrast, male mice did not show any differences in bone mineral density at 11 weeks, 12 months, or 18 months, compared to controls (Suppl. Fig. 4A-C). In addition, no differences in body mass composition were seen in male mutant and control mice at 11 weeks, 12 months, and 18 months of age (Suppl. Fig. 5A1-C2).

**Mig-6 overexpressing mice have healthy articular cartilage during skeletal maturity** We next examined articular cartilage morphology in 11-week-old mutant and control mice using toluidine blue stained paraffin frontal knee sections (Fig. 3A-B). The average thickness of the calcified articular cartilage and non-calcified articular cartilage in the lateral femoral condyle (LFC), lateral tibial plateau (LTP), medial femoral condyle (MFC), and medial tibial plateau (MTP) from control and *Mig-6<sup>over/over</sup>* male (Fig. 3 C-D) and female (Suppl. Fig. 6A-D) mice did not show statistically significant differences. Histological

analyses of knee sections from male and female mice did not show any loss of proteoglycan, fibrillation or erosion in the articular cartilage of mutant mice.

### **Overexpression of Mig-6 in cartilage induces an osteoarthritis-like phenotype in mice during aging**

Since aging is a primary risk factor in OA (49), we next examined knee joints in 12 and 18 month-old control and *Mig-6<sup>over/over</sup>* mice. Toluidine blue stained sections were evaluated by two blinded observers, using OARSI recommendations (47). At 12 month of age, male control mice showed minor signs of cartilage damage, such as loss of proteoglycan staining, but no significant structural degeneration (Fig. 4A). However, seven of nine *Mig-6<sup>over/over</sup>* male mice showed more extensive cartilage damage in their medial side (erosion to the calcified layer lesion for 25% to 50% of the medial quadrant) (Fig. 4B). OARSI scoring confirmed increased OA-like damage in mutant mice (Fig. 4C). Similarly, at 18 months of age the male control group showed minimal cartilage degeneration in 3 of 6 mice (Suppl. Fig. 7A-B). *Mig-6<sup>over/over</sup>* male mice showed more severe cartilage erosion in the medial tibial plateau in 3/6 animals. This result was again supported by significantly increased OARSI cartilage damage scores (Suppl. Fig. 7C). Moreover, for the female group at 12 months, control mice did not show cartilage damage. However, *Mig-6<sup>over/over</sup>* female mice showed sign of OA-like cartilage damage in 3/8 animals (Suppl. Fig. 8A-C). In addition, at 18 months of age, female control mice showed healthy cartilage, and 3/8 *Mig-6<sup>over/over</sup>* female mice showed some proteoglycan loss and cartilage degeneration on the medial side (Suppl. Fig. 9A-C).

### **Overexpression of *Mig-6* decreases Sox9 expression**

During chondrogenesis, the transcription factor SOX9 is required for cartilage formation and normal expression of collagen and aggrecan (50). Sagittal and frontal sections of paraffin embedded knees from post-natal day 0 (P0), 6 weeks-old, 11 weeks-old, 12 months and 18 months male mice were used for SOX9 immunostaining. At P0, nuclear SOX9 expression was observed in the resting and proliferative zone of the growth plate in both genotypes (Fig. 5A, B). Cell density was not different between genotypes (Fig. 5C). In control mice, 78 % of chondrocytes were positive for SOX 9 immunostaining, while the proportion of positive cells was only 53 % in *Mig-6<sup>over/over</sup>* mice (Fig 5D). At 6 weeks-old the total cell number in control male and *Mig-6<sup>over/over</sup>* mice is similar (Fig. 5G), but the percentage of SOX9 positive cells was decreased in mutant mice (Fig 5H). A similar phenotype was present at 11 weeks (Suppl. Fig.10A-B). At 12 months of age, SOX9 is present more in the lateral side (LTP and LFC) than the medial side (MTP and MFC) in both strains, with a few positive cells present in the medial side of the control strain. On the other hand, *Mig-6<sup>over/over</sup>* mice showed fewer SOX9-positive cells on the medial side due the articular cartilage damage (Suppl. Fig. 11A-B). Similar results were found at 18 months of age in *Mig-6<sup>over/over</sup>*, with decreased SOX9 immunostaining in their medial side compared to the control (data not shown). For all ages, negative controls did not show staining in chondrocytes.

### **Overexpression of Mig-6 decreases expression of lubricin**

Lubricin (aka PRG4/superficial zone protein) is a proteoglycan that plays an important role as lubricant in the joint (51). EGFR signaling is crucial for the cartilage lubrication function and regulates the induction of *Prg4* expression which is necessary for smooth movement (31,32). Immunohistochemistry for Lubricin in 11week-old (Fig 6A-D) and at 12 months-old animals demonstrated less staining in the superficial zone of the medial side of *Mig-6<sup>over/over</sup>* mice than in the control group (Suppl. Fig. 12A-B).

### **MMP13 immunostaining in Mig-6-overexpressing and control mice**

Matrix metalloproteinase (MMP13) is highly expressed in OA (52,53). Frontal sections of knees from 12- and 18-month-old control and *Mig-6<sup>over/over</sup>* male mice were used for MMP13 immunohistochemistry. At 12 months, pericellular staining was observed in the lateral articular cartilage of male mice from both genotypes, along with the expected subchondral bone staining (Suppl. Fig. 13A-B). Less staining was observed on the medial side of control mice while advanced cartilage degeneration in mutant mice precluded staining. Negative controls did not show staining in cartilage or subchondral bone. Articular cartilage from 18 months-old mice showed similar staining patterns and intensity of MMP13 immunostaining in the lateral side of both genotypes, however in the medial side of *Mig-6<sup>over/over</sup>* mice, MMP13 staining is seen on the cartilage surface (lesion sites) and also observed in the subchondral bone (data not shown).

## **Discussion**

The maintenance of articular cartilage homeostasis relies on a dynamic equilibrium involving growth factors (54), genetics (55), mechanical forces (56), obesity and injury, that all play a role in the onset of osteoarthritis (57). Better understanding of the underlying molecular mechanism is required to design therapies for preventing progression of OA. Recent studies from our laboratory and others have identified the epidermal growth factor receptor (EGFR) and Mig-6 as possible mediators of articular cartilage homeostasis (31,34,40,58). *Mig-6* is a cytosolic protein and negative feedback regulator of EGFR signalling (59); thus, *Mig-6* can be a potential tumor suppressor (41,60–63). In addition, whole body knockout of the *Mig-6* gene in mice results in degenerative joint disease (37). We also have shown previously that constitutive cartilage-specific deletion of *Mig-6* (*Mig-6* KO) results in increased articular cartilage thickness and cell density in the joints of 12 week-old mice (40). Cartilage-specific *Mig-6* KO mice show the same anabolic effect in joint cartilage at 21 months of age (unpublished).

Previous research demonstrates that Mig-6 overexpression acts as a negative feedback regulator of EGFR-ERK signalling (41), however these studies did not yet analyze joint tissues. Since our studies suggest dosage- and/or context-specific roles of EGFR signaling in joint homeostasis and OA (34), we now examined whether overexpression of Mig-6 alters these processes. Here, we report that cartilage-specific constitutive overexpression of *Mig-6* did not cause cartilage degeneration in young mice, but early onset OA in middle aged mice. While we observed some effects of Mig-6 overexpression on bone length and weight, these effects were subtle and not accompanied by major morphological or histological changes in growth plate cartilage, overall skeletal morphology, or body composition. A previous study

showed that deletion of EGFR in bone tissue (*Col1-Cre Egfr<sup>Wa5/f</sup>*) resulted in shorter femurs compared to wild-type mice (64), consistent with our findings. The EGFR network is essential during long bone development, since previous studies have shown that EGFR- or TGF $\alpha$ -deficient mice exhibit a widened zone of hypertrophic chondrocytes (23,65). Moreover, Qin and colleagues have shown that administration of the EGFR inhibitor, gefitinib, into 1-month-old rats results in an enlarged hypertrophic zone due down-regulation of MMP-9, -13 and -14 (30). Together these data suggest a critical role of EGFR during endochondral ossification and elucidate downstream mechanism of EGFR (66). Further research is required to provide more evidence of EGFR/*Mig-6<sup>over/over</sup>* signalling during bone formation, but many of these effects are relatively subtle and transient, and likely unrelated to the much more severe phenotypes observed later. Histologically, our findings showed that mice with cartilage-specific *Mig-6* overexpression showed healthy articular cartilage with no significant difference in articular cartilage thickness from control group at the ages of 6 weeks and 11 weeks. However, *Mig-6<sup>over/over</sup>* mice developed severe degeneration of articular cartilage with aging. More prevalent, the knee joints of *Mig-6<sup>over/over</sup>* male mice showed significantly advanced cartilage degeneration. The same pattern, but with more severe damage, was seen in 18-month-old mice. As previously described, sex hormones play a role in OA disease where male mice develop more severe OA (67). SOX9 is crucial in chondrogenesis during endochondral bone formation, articular cartilage development and cartilage homeostasis (50). Previous *in vivo* models using cartilage (*Col2-Cre* or limb mesenchyme (*Prx1*)-*Cres* specific ablation of *Mig-6* showed increased expression of SOX9 in the articular cartilage. Consistent with these data, we show that percentage of SOX9-positive chondrocytes was decreased in knee joints of 6 and 11-week-old male *Mig-6<sup>over/over</sup>* mice compared to controls, despite the absence of histological defects in articular cartilage. The percentage of SOX9-expressing cells was also reduced in *Mig-6<sup>over/over</sup>* mice at later ages. However, our previous *in vitro* studies suggested that TGF $\alpha$  suppresses expression of anabolic genes such as Sox9, type II collagen and aggrecan in primary chondrocytes (21). A potential explanation for these conflicting results is the context-specific role of EGFR signaling in cartilage, as discussed previously (34); this pathway can both promote cartilage degeneration and confer protection of cartilage, depending on context. Another potential explanation is the difference between *in vivo* and *in vitro* experiments. Our data from the current study suggest that reduction in Sox9 expression precedes the degeneration of articular chondrocytes in our mutant mice. In addition, we observed decreased expression of lubricin/PRG4 in these joints, which might also contribute to the observed joint pathologies. PRG4 has been shown to be regulated by EGFR signaling before (31,32), in support of our findings. While the EGFR is the best characterized substrate of Mig-6, other substrates have been described. Mig-6 binds to different proteins such as the cell division control protein 42 homolog (Cdc42) (68), proto-oncoprotein (c-Abl) (69), and the hepatocyte growth factor receptor (c-Met) (70). While we cannot exclude that deregulation of these other substrates contributes to the observed phenotypes, the similarities of defects in our mice with those seen upon cartilage-specific deletion of EGFR suggest that decreased EGFR signaling is the main cause for the advanced OA observed in our mutant mice. Nevertheless, it will be important to determine whether signaling through cMet and other pathways is altered as well.

Future studies will include examination of Mig-6-overexpressing mice in other models of OA, such as the post-traumatic model of DMM (destabilization of the medial meniscus) surgery. As discussed above, the role of the EGFR/Mig-6 pathway in OA is context-specific. Thus, we cannot extrapolate from our aging model to all forms of OA. In addition, the role of Mig-6 in human OA will require further studies. While there is plenty of evidence for crucial roles of the EGFR pathway in human OA, and Mig-6 is a crucial regulator of this pathway, more direct analyses of this role in human cartilage is required (21,71,72).

Mig-6 expression is heavily regulated. While its expression in human OA has not been studied thoroughly, one can easily imagine upregulation by a number of biochemical (such as EGFR and other growth factors, as in other tissues) or biomechanical factors. Mig-6 overexpression has been demonstrated in OA cartilage in dogs (38), suggesting that the same could occur in human OA. More generally, the EGFR pathway, through which Mig-6 primarily acts, has been shown to be deregulated in human OA in several studies (21,34,72). Thus, the current study is highly relevant to the pathogenesis of human OA.

## **Conclusion**

In conclusion, we show for the first time that cartilage-specific Mig-6 overexpression in mice results in reduced EGFR activity in chondrocytes, reduced SOX9 and PRG4 expression, and accelerated development of OA. These data highlight the important and context-specific role of the EGFR-Mig-6 signaling pathway in joint homeostasis and point towards potential targeting of this pathway for OA therapy.

## **Declarations**

### **Ethics approval and consent to participate**

All experiments were conducted under supervision of the Animal Care Committee (ACC) at the University of Western Ontario under the Animal Use Protocol (AUP) 2019-035:1: titled “The Regulation of Endochondral Bone Growth by Hormones”.

### **Consent for publication**

Not applicable.

### **Availability of data and material**

The dataset of the current manuscript is available upon request from the corresponding author.

### **Competing interests**

The authors declare that they have no competing interests.

### **Funding**

This study was funded by fellowship from Conselho Nacional de Desenvolvimento Científico e Tecnológico (CNPq)/Brazil (201342/2014-6) to M.B. Also, F.B. is supported by a grant from the Canadian Institutes of Health Research (Grant #332438). F.B. holds the Canada Research Chair in Musculoskeletal Research.

### **Authors' contributions**

All authors were involved in revising the article or drafting it critically for important intellectual content, all authors read and approved the final manuscript to be published. Dr. Beier had full access to all of the data in the study and takes responsibility for the integrity of the data and the accuracy of the data analysis.

### **Study conception and design**

Bellini, Beier.

### **Acquisition of data**

Bellini, Miranda-Rodrigues.

### **Analysis and interpretation of data**

Bellini, Pest, Miranda-Rodrigues, Qin, Jeong, Beier.

### **Acknowledgements**

We would like to thank Julia Bowering for kindly performing articular cartilage sectioning.

## **Abbreviations**

*Acan* Aggrecan gene

BMD Bone Mineral Density

c-Abl Non-receptor Tyrosine Kinase Proto-oncoprotein

CAGGS Chicken Beta Actin-Cytomegalovirus Hybrid

Cdc42 Cell Division Control Protein 42

cDNA Complementary DNA

c-Met Hepatocyte Growth Factor Receptor

*Col2a1* Type II Collagen gene

ECM Extracellular Matrix

EGFR Epidermal Growth Factor Receptor

ERK1/2 Extracellular Signal-Regulated Kinase 1 and 2

ERRFI1 ErbB Receptor Feedback Inhibitor 1

*Gadph* Glyceraldehyde 3-Phosphate Dehydrogenase gene

GE General Electric

HRP Horseradish Peroxidase

HU Hounsfield Units

IGF-1 Insulin Growth Factor 1

KO Knockout

LFC Lateral Femoral Condyle

LSL "Stop Cassette" flanked by LoxP (LoxP-Stop Cassette-LoxP)

LTP Lateral Tibial Plateau

Lubricin PRG4/Superficial Zone Protein

MFC Medial Femoral Condyle

*Mig-6* Mitogen-Inducible Gene 6; RALT; Gene 33

MMP13 Matrix Metalloproteinase 13

OA Osteoarthritis

OARSI Osteoarthritis Research Society International

P0 Newborn Mouse (Post Natal day 0)

PBS Phosphate Buffered Solution

pEGFR Phosphorylated Epidermal Growth Factor Receptor

PI3K Phosphoinositide 3-Kinase

ROI Region of Interest

SB3 Cortical Bone-Mimicking Calibrator

SOX9 Sex-determining-region-Y Box 9

TGF $\alpha$  Transforming Growth Factor Alpha

$\mu$ CT Micro-Computerized Tomography

## References

1. Woolf, A. D. & Pfleger, B. Burden of major musculoskeletal conditions. *Bull. World Health Organ.***81**, 646–56 (2003).
2. Kramer, W. C., Hendricks, K. J. & Wang, J. Pathogenetic mechanisms of posttraumatic osteoarthritis: Opportunities for early intervention. *Int. J. Clin. Exp. Med.* (2011).
3. Ruan, M. Z. *et al.* Treatment of osteoarthritis using a helper-dependent adenoviral vector retargeted to chondrocytes. *Mol. Ther. – Methods Clin. Dev.***3**, 16008 (2016).
4. Sokolove, Jeremy and Lepus, C. M. Role of inflammation in the pathogenesis of osteoarthritis: latest findings and interpretations. *Ther Adv Musculoskel Dis***5**, 77–94 (2013).
5. Mcalindon, T. E. *et al.* OARSI guidelines for the non-surgical management of knee osteoarthritis. *Osteoarthr. Cartil.***22**, 363–388 (2014).
6. Hunter, D. J. Osteoarthritis. *Best Pract. Res. Clin. Rheumatol.***25**, 801–814 (2011).
7. Driban, J. B., Sitler, M. R., Barbe, M. F. & Balasubramanian, E. Is osteoarthritis a heterogeneous disease that can be stratified into subsets? *Clin. Rheumatol.***29**, 123–131 (2010).
8. Man, G. S. & Mologhianu, G. Osteoarthritis pathogenesis - a complex process that involves the entire joint. *J. Med. Life***7**, 37–41 (2014).
9. Felson, D. T. Osteoarthritis as a disease of mechanics. *Osteoarthr. Cartil.***21**, 10–5 (2013).
10. Fox, A. J. S. *et al.* The Basic Science of Articular Cartilage: Structure, Composition, and Function. *Sports Health***1**, 461–8 (2009).
11. Saha, A. K. & Kohles, S. S. A cell-matrix model of anabolic and catabolic dynamics during cartilage biomolecule regulation. *Int. J. Comput. Healthc.***1**, 214–228 (2012).
12. Goldring, M. B. *et al.* Cartilage homeostasis in health and rheumatic diseases. *Arthritis Res. Ther.***11**, 224 (2009).
13. Tsang, K. Y., Tsang, S. W., Chan, D. & Cheah, K. S. E. The chondrocytic journey in endochondral bone growth and skeletal dysplasia. *Birth Defects Res. Part C Embryo Today Rev.***102**, 52–73 (2014).
14. Gilbert, A. M., Bikker, J. A. & O’Neil, S. V. Advances in the development of novel aggrecanase inhibitors. *Expert Opin. Ther. Pat.***21**, 1–12 (2011).
15. Parks, W. C., Wilson, C. L. & López-Boado, Y. S. Matrix metalloproteinases as modulators of inflammation and innate immunity. *Nat. Rev. Immunol.***4**, 617–629 (2004).

16. Yoon, Y. M. *et al.* Epidermal growth factor negatively regulates chondrogenesis of mesenchymal cells by modulating the protein kinase C-alpha, Erk-1, and p38 MAPK signaling pathways. *J. Biol. Chem.***275**, 12353–9 (2000).
17. Fortier, L. A., Barker, J. U., Strauss, E. J., McCarrel, T. M. & Cole, B. J. The role of growth factors in cartilage repair. *Clin. Orthop. Relat. Res.***469**, 2706–15 (2011).
18. Kraan, P. M. van der. Differential Role of Transforming Growth Factor-beta in an Osteoarthritic or a Healthy Joint. *J. Bone Metab.***25**, 65 (2018).
19. Gamer, L. W. *et al.* The Role of *Bmp2* in the Maturation and Maintenance of the Murine Knee Joint. *J. Bone Miner. Res.***33**, 1708–1717 (2018).
20. Wei, F.-Y., Lee, J. K., Wei, L., Qu, F. & Zhang, J.-Z. Correlation of insulin-like growth factor 1 and osteoarthritic cartilage degradation: a spontaneous osteoarthritis in guinea-pig. *Eur. Rev. Med. Pharmacol. Sci.***21**, 4493–4500 (2017).
21. Appleton, C. T. G., Usmani, S. E., Bernier, S. M., Aigner, T. & Beier, F. Transforming growth factor  $\alpha$  suppression of articular chondrocyte phenotype and Sox9 expression in a rat model of osteoarthritis. *Arthritis Rheum.***56**, 3693–3705 (2007).
22. Appleton, C. T. G. *et al.* Global analyses of gene expression in early experimental osteoarthritis. *Arthritis Rheum.***56**, 3693–705 (2007).
23. Usmani, S. E. *et al.* Transforming growth factor alpha controls the transition from hypertrophic cartilage to bone during endochondral bone growth. *Bone***51**, 131–141 (2012).
24. Appleton, C. T. G. *et al.* Reduction in disease progression by inhibition of transforming growth factor  $\alpha$ -CCL2 signaling in experimental posttraumatic osteoarthritis. *Arthritis Rheumatol. (Hoboken, N.J.)***67**, 2691–701 (2015).
25. Usmani, S. E. *et al.* Context-specific protection of TGF $\alpha$  null mice from osteoarthritis. *Sci. Rep.***6**, 30434 (2016).
26. Cui, G. *et al.* Association of Common Variants in TGFA with Increased Risk of Knee Osteoarthritis Susceptibility. *Genet. Test. Mol. Biomarkers***21**, 586–591 (2017).
27. Zengini, E. *et al.* Genome-wide analyses using UK Biobank data provide insights into the genetic architecture of osteoarthritis. *Nat. Genet.* **2018** 1 (2018). doi:10.1038/s41588-018-0079-y
28. Appleton, C. T. G., Usmani, S. E., Mort, J. S. & Beier, F. Rho/ROCK and MEK/ERK activation by transforming growth factor- $\alpha$  induces articular cartilage degradation. *Lab. Investig.***90**, 20–30 (2010).
29. Wang, K., Yamamoto, H., Chin, J. R., Werb, Z. & Vu, T. H. Epidermal growth factor receptor-deficient mice have delayed primary endochondral ossification because of defective osteoclast recruitment. *J. Biol. Chem.***279**, 53848–56 (2004).
30. Zhang, X. *et al.* The critical role of the epidermal growth factor receptor in endochondral ossification. *J. Bone Miner. Res.***26**, 2622–33 (2011).
31. Jia, H. *et al.* EGFR signaling is critical for maintaining the superficial layer of articular cartilage and preventing osteoarthritis initiation. *Proc. Natl. Acad. Sci. U. S. A.***113**, 14360–14365 (2016).

32. Shepard, J. B., Jeong, J.-W., Maihle, N. J., O'Brien, S. & Dealy, C. N. Transient anabolic effects accompany epidermal growth factor receptor signal activation in articular cartilage in vivo. *Arthritis Res. Ther.***15**, R60 (2013).
33. Zhang, X. *et al.* Reduced EGFR signaling enhances cartilage destruction in a mouse osteoarthritis model. *Bone Res.***2**, 14015 (2014).
34. Qin, L. & Beier, F. EGFR Signaling: Friend or Foe for Cartilage? *JBMR Plus***3**, e10177 (2019).
35. Jin, N., Gilbert, J. L., Broaddus, R. R., Demayo, F. J. & Jeong, J.-W. Generation of a Mig-6 conditional null allele. *Genesis***45**, 716–21 (2007).
36. Frosi, Y. *et al.* A two-tiered mechanism of EGFR inhibition by RALT/MIG6 via kinase suppression and receptor degradation. *J. Cell Biol.***189**, 557–71 (2010).
37. Zhang, Y.-W. *et al.* Targeted disruption of Mig-6 in the mouse genome leads to early onset degenerative joint disease. *Proc. Natl. Acad. Sci. U. S. A.***102**, 11740–5 (2005).
38. Mateescu, R. G., Todhunter, R. J., Lust, G. & Burton-Wurster, N. Increased MIG-6 mRNA transcripts in osteoarthritic cartilage. *Biochem. Biophys. Res. Commun.***332**, 482–6 (2005).
39. Joiner, D. M. *et al.* Accelerated and increased joint damage in young mice with global inactivation of mitogen-inducible gene 6 after ligament and meniscus injury. *Arthritis Res. Ther.***16**, R81 (2014).
40. Pest, M. A., Russell, B. A., Zhang, Y.-W., Jeong, J.-W. & Beier, F. Disturbed cartilage and joint homeostasis resulting from a loss of mitogen-inducible gene 6 in a mouse model of joint dysfunction. *Arthritis Rheumatol. (Hoboken, N.J.)***66**, 2816–27 (2014).
41. Kim, T. H. *et al.* Mig-6 suppresses endometrial cancer associated with pten deficiency and ERK activation. *Cancer Res.***74**, 7371–7382 (2014).
42. Terpstra, L. *et al.* Reduced chondrocyte proliferation and chondrodysplasia in mice lacking the integrin-linked kinase in chondrocytes. *J. Cell Biol.***162**, (2003).
43. Ratneswaran, A. *et al.* Nuclear receptors regulate lipid metabolism and oxidative stress markers in chondrocytes. *J. Mol. Med. (Berl)***95**, 431–444 (2017).
44. Schneider, C. A., Rasband, W. S. & Eliceiri, K. W. NIH Image to ImageJ: 25 years of image analysis. *Nat. Methods***9**, 671–675 (2012).
45. Beaucage, K. L., Pollmann, S. I., Sims, S. M., Dixon, S. J. & Holdsworth, D. W. Quantitative in vivo micro-computed tomography for assessment of age-dependent changes in murine whole-body composition. *Bone Reports***5**, 70–80 (2016).
46. White, D. R. Tissue substitutes in experimental radiation physics. *Med. Phys.***5**, 467–479 (1978).
47. Glasson, S. S., Chambers, M. G., Van Den Berg, W. B. & Little, C. B. The OARSI histopathology initiative – recommendations for histological assessments of osteoarthritis in the mouse. *Osteoarthr. Cartil.***18**, S17–S23 (2010).
48. Ratneswaran, A. *et al.* Peroxisome proliferator-activated receptor  $\delta$  promotes the progression of posttraumatic osteoarthritis in a mouse model. *Arthritis Rheumatol. (Hoboken, N.J.)***67**, 454–64 (2015).

49. Zhang, M., Egan, B. & Wang, J. Epigenetic mechanisms underlying the aberrant catabolic and anabolic activities of osteoarthritic chondrocytes. *Int. J. Biochem. Cell Biol.***67**, 101–9 (2015).
50. Lefebvre, V., Dvir-Ginzberg, M. & Hebrew, : SOX9 and the many facets of its regulation in the chondrocyte lineage HHS Public Access. *Connect Tissue Res***58**, 2–14 (2017).
51. Waller, K. A. *et al.* Role of lubricin and boundary lubrication in the prevention of chondrocyte apoptosis. *Proc. Natl. Acad. Sci. U. S. A.***110**, 5852–7 (2013).
52. Wang, M. *et al.* MMP13 is a critical target gene during the progression of osteoarthritis. *Arthritis Res. Ther.***15**, R5 (2013).
53. Blaney Davidson, E. N. *et al.* Correction: Increase in ALK1/ALK5 Ratio as a Cause for Elevated MMP-13 Expression in Osteoarthritis in Humans and Mice. *J. Immunol.***185**, 2629–2629 (2010).
54. Mariani, E., Pulsatelli, L. & Facchini, A. Signaling pathways in cartilage repair. *Int. J. Mol. Sci.***15**, 8667–98 (2014).
55. Lee, A. *et al.* A Current Review of Molecular Mechanisms Regarding Osteoarthritis and Pain. *Gene***527**, 440–447 (2013).
56. Bader, D. L., Salter, D. M. & Chowdhury, T. T. Biomechanical influence of cartilage homeostasis in health and disease. *Arthritis***2011**, 979032 (2011).
57. Richmond, S. A. *et al.* Are Joint Injury, Sport Activity, Physical Activity, Obesity, or Occupational Activities Predictors for Osteoarthritis? A Systematic Review. *J. Orthop. Sport. Phys. Ther.***43**, 515-B19 (2013).
58. Zhang, X. *et al.* Reduced EGFR signaling enhances cartilage destruction in a mouse osteoarthritis model. *Bone Res.***2**, 14015 (2014).
59. Hackel, P. O., Gishizky, M. & Ullrich, A. Mig-6 Is a Negative Regulator of the Epidermal Growth Factor Receptor Signal. *Biol. Chem.***382**, 1649–62 (2001).
60. Maity, T. K. *et al.* Loss of MIG6 Accelerates Initiation and Progression of Mutant Epidermal Growth Factor Receptor-Driven Lung Adenocarcinoma. *Cancer Discov.***5**, 534–49 (2015).
61. Li, Z. *et al.* Downregulation of Mig-6 in nonsmall-cell lung cancer is associated with EGFR signaling. *Mol. Carcinog.***51**, 522–34 (2012).
62. Zhang, Y.-W. *et al.* Evidence that MIG-6 is a tumor-suppressor gene. *Oncogene***26**, 269–276 (2007).
63. Sasaki, M., Terabayashi, T., Weiss, S. M. & Ferby, I. The Tumor Suppressor MIG6 Controls Mitotic Progression and the G2/M DNA Damage Checkpoint by Stabilizing the WEE1 Kinase. *Cell Rep.***24**, 1278–1289 (2018).
64. Zhang, X. *et al.* Epidermal growth factor receptor plays an anabolic role in bone metabolism in vivo. *J. Bone Miner. Res.***26**, 1022–34 (2011).
65. Sibilias, M. *et al.* Correction: Mice humanised for the EGF receptor display hypomorphic phenotypes in skin, bone and heart. *Development***143**, 4755–4755 (2017).
66. Zhang, X. *et al.* Epidermal Growth Factor Receptor (EGFR) Signaling Regulates Epiphyseal Cartilage Development through  $\beta$ -Catenin-dependent and -independent Pathways. *J. Biol. Chem.***288**, 32229–

32240 (2013).

67. Ma, H.-L. *et al.* Osteoarthritis severity is sex dependent in a surgical mouse model. *Osteoarthr. Cartil.***15**, 695–700 (2007).
68. Jiang, X. *et al.* Inhibition of Cdc42 is essential for Mig-6 suppression of cell migration induced by EGF. *Oncotarget* (2016). doi:10.18632/oncotarget.10205
69. Hopkins, S. *et al.* Mig6 is a sensor of EGF receptor inactivation that directly activates c-Abl to induce apoptosis during epithelial homeostasis. *Dev. Cell***23**, 547–59 (2012).
70. Pante, G. *et al.* Mitogen-inducible gene 6 is an endogenous inhibitor of HGF/Met-induced cell migration and neurite growth. *J. Cell Biol.***171**, 337–48 (2005).
71. Castaño-Betancourt, M. C. *et al.* Novel Genetic Variants for Cartilage Thickness and Hip Osteoarthritis. *PLoS Genet.***12**, e1006260 (2016).
72. Sun, H. *et al.* Gefitinib for Epidermal Growth Factor Receptor Activated Osteoarthritis Subpopulation Treatment. *EBioMedicine***32**, 223–233 (2018).

## Figures

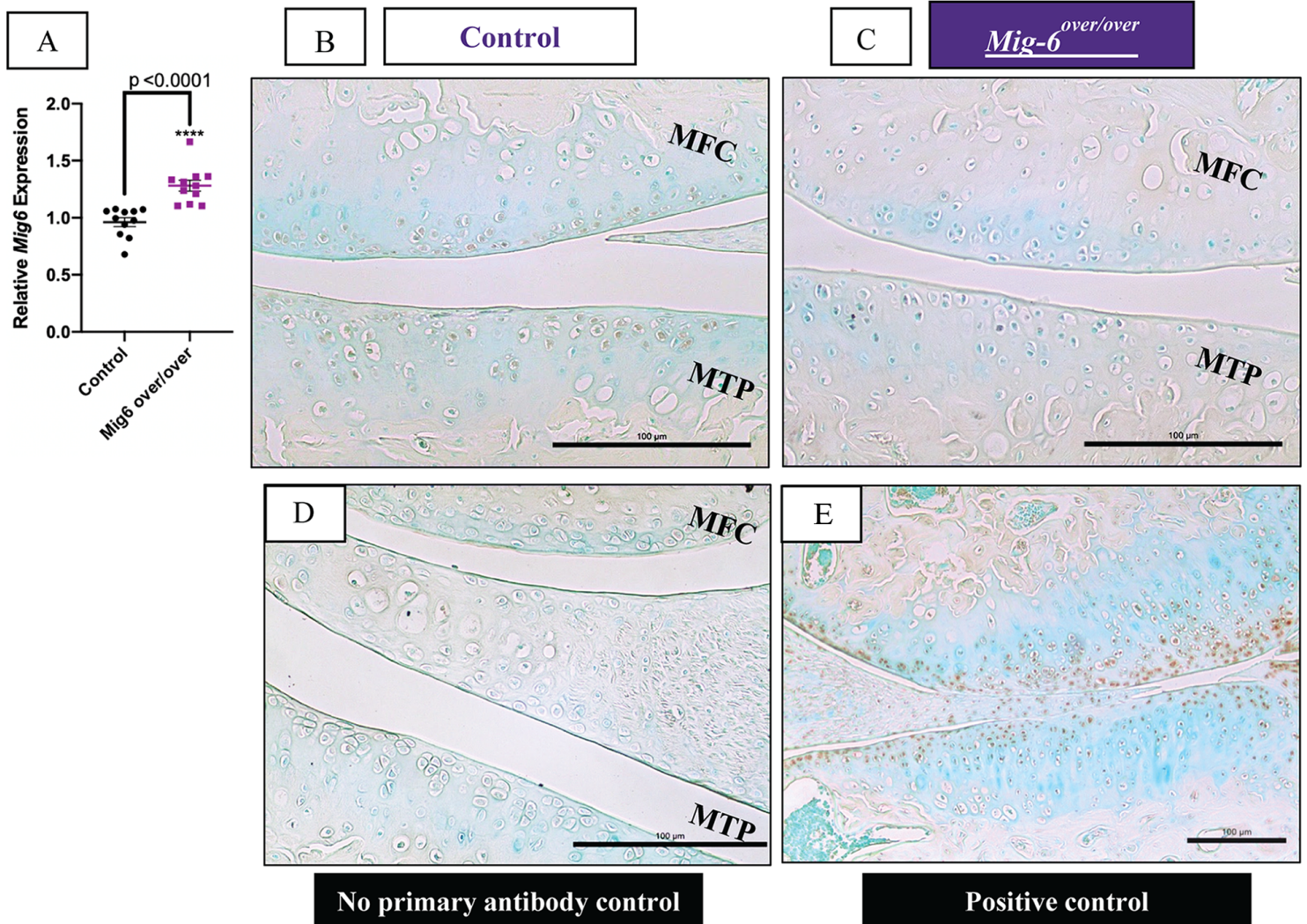


**Figure 1**

Mig-6 mRNA and EGFR protein expression in the articular cartilage of cartilage specific Mig-6 overexpressing mice. (A) Levels of Mig-6 mRNA were determined by qRT-PCR analysis on P0 epiphysis. Individual data points presented with mean  $\pm$  SEM ( $P < 0.05$ ). Data analyzed by two tailed student t-tests from 11 mice per group. (B) Immunostaining of phosphorylated epidermal growth factor receptor (pEGFR; Tyr-1173) in the knee joints of 11-week-old control and (C) Mig-6over/over (Mig-6over/overCol2a1-Cre+/-) is decreased in response to increased Mig-6 levels. Frontal sections of mouse articular cartilage incubated without primary antibody, as negative control, exhibited no staining (D). Cartilage-specific Mig-6 KO mice served as positive control (E). N=5 mice/genotyping. MFC = medial femoral condyle and MTP = medial tibial plateau. Scale bar = 100 $\mu$ m.

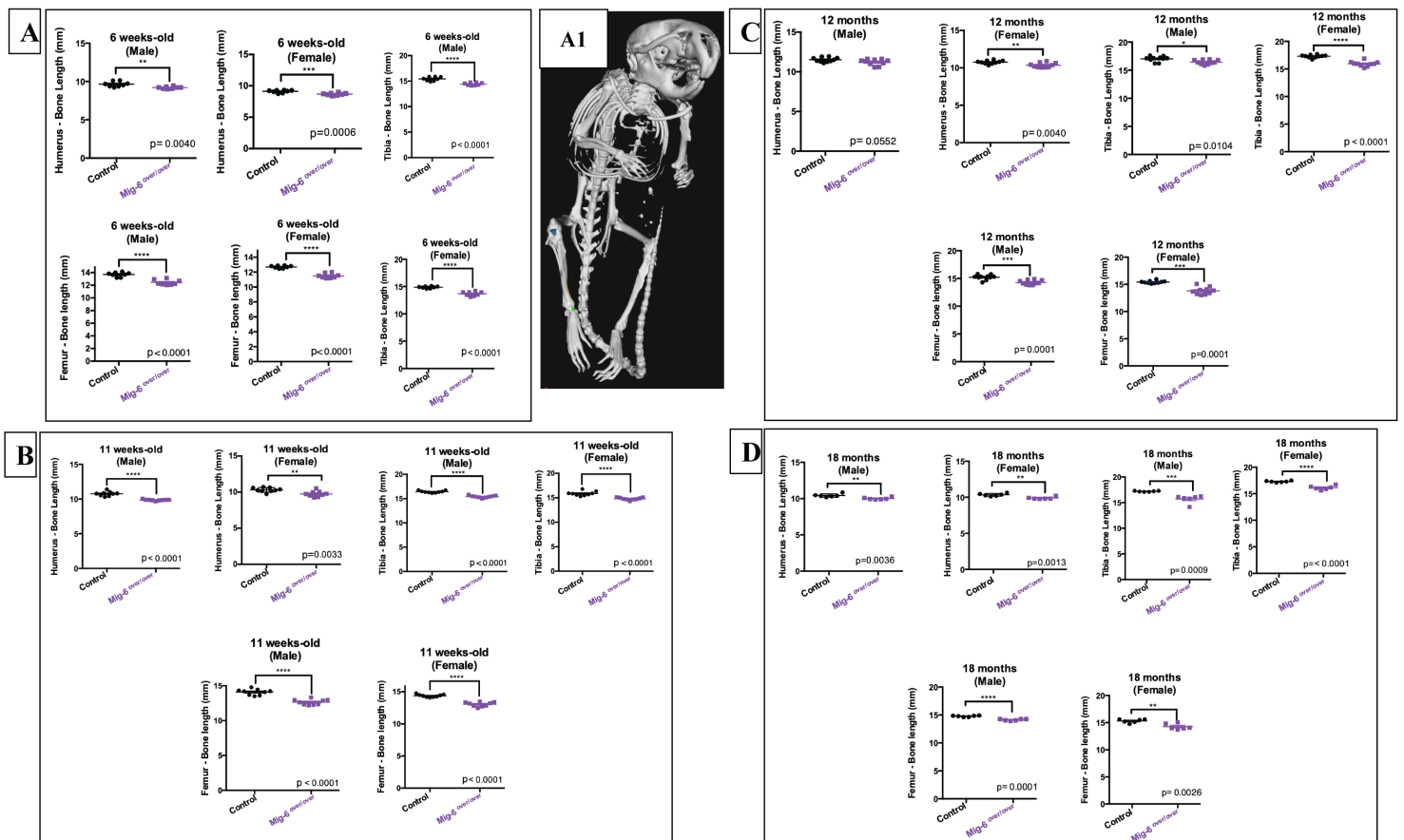


**Figure 2**

Long bones of Mig-6 overexpressing mice are significantly shorter than control long bone during growth and aging. The lengths of right humeri, tibiae and femora were measured on microCT scans of mice at different ages using GE MicroView software. (A) 6 weeks-old male and female control and Mig-6 overexpressing mice. (B) 11 weeks-old male and female control and Mig-6 overexpressing mice. (C) 12 months-old male and female control and Mig-6 overexpressing mice. (D) 18 months-old male and female control and Mig-6 overexpressing mice. (A1) Representative 3D isosurface reconstructions of 100 $\mu$ m/voxel  $\mu$ CT scans. There were statistically significant differences between control and Mig-

6over/over male and female groups. Individual data points presented with mean  $\pm$  SEM ( $P < 0.05$ ). Data analyzed by two tailed student t-tests from 6-12 mice per group (age/gender).

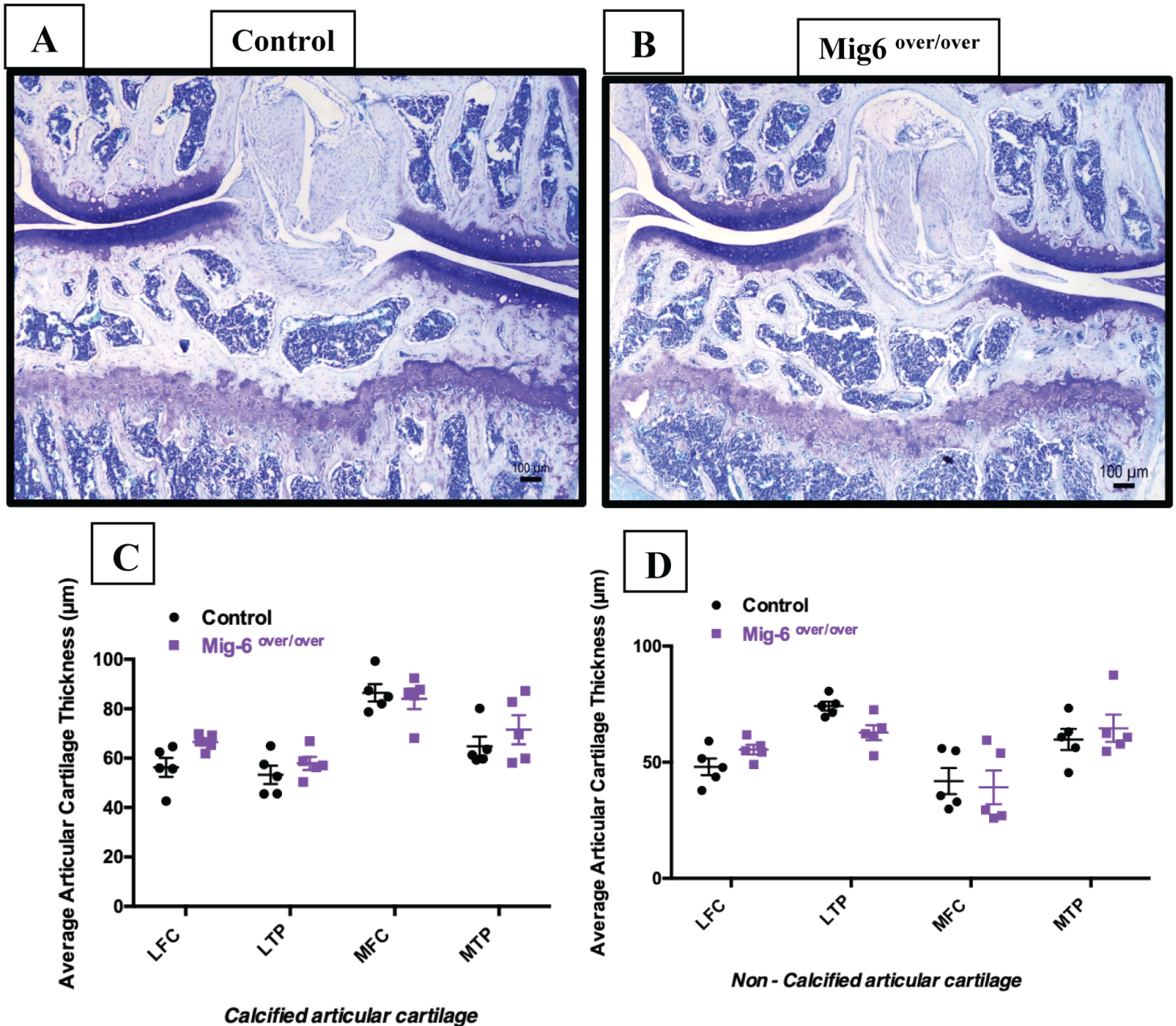


**Figure 3**

Articular cartilage from 11 weeks-old Mig-6over/over male mice appeared healthy at skeletal maturity. Representative (n=5/group, toluidine blue) stained frontal sections of knee joints from 11-week-old control (A) and Mig-6over/over (B) mice. Mig-6 overexpressing mice show similar articular cartilage thickness when compared to controls at 11 weeks of age. The average thickness of the calcified articular cartilage (C) and non-calcified articular cartilage (D) in the lateral femoral condyle (LFC), lateral tibial plateau (LTP), medial femoral condyle (MFC), medial tibial plateau (MTP) was measured. Individual data points presented with mean  $\pm$  SEM. Data analyzed by two-way ANOVA (95% CI) with Bonferroni post-hoc test. Scale bar = 100µm.

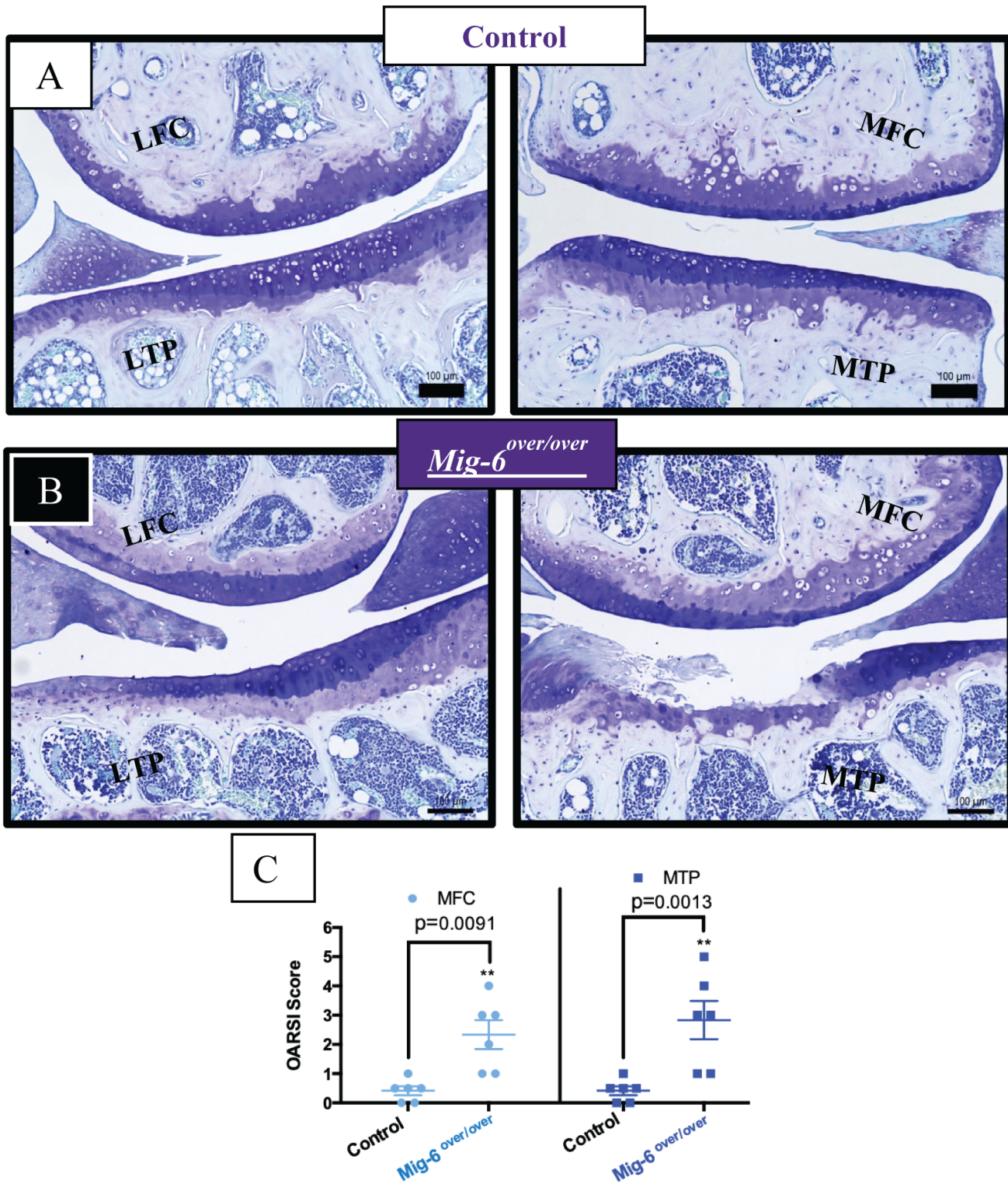


**Figure 4**

12 months old Mig-6over/over male mice develop OA-like cartilage degeneration. Toluidine Blue stained sections of knee joints from 12-month male control (A) and Mig-6over/over (B) mice were evaluated for cartilage damage following OARSI histopathological scale on two quadrants of the knee: MFC = medial femoral condyle, MTP = medial tibial plateau. OARSI based cartilage degeneration scores are significantly higher in the MFC and MTP of Mig-6 overexpressing mice, corresponding to the increased

damage observed histologically (C). Data analyzed by two-way ANOVA with Bonferroni's multiple comparisons test. Individual data points presented with mean  $\pm$  SEM. All scale bars =100  $\mu$ m. N = 9 mice/group.

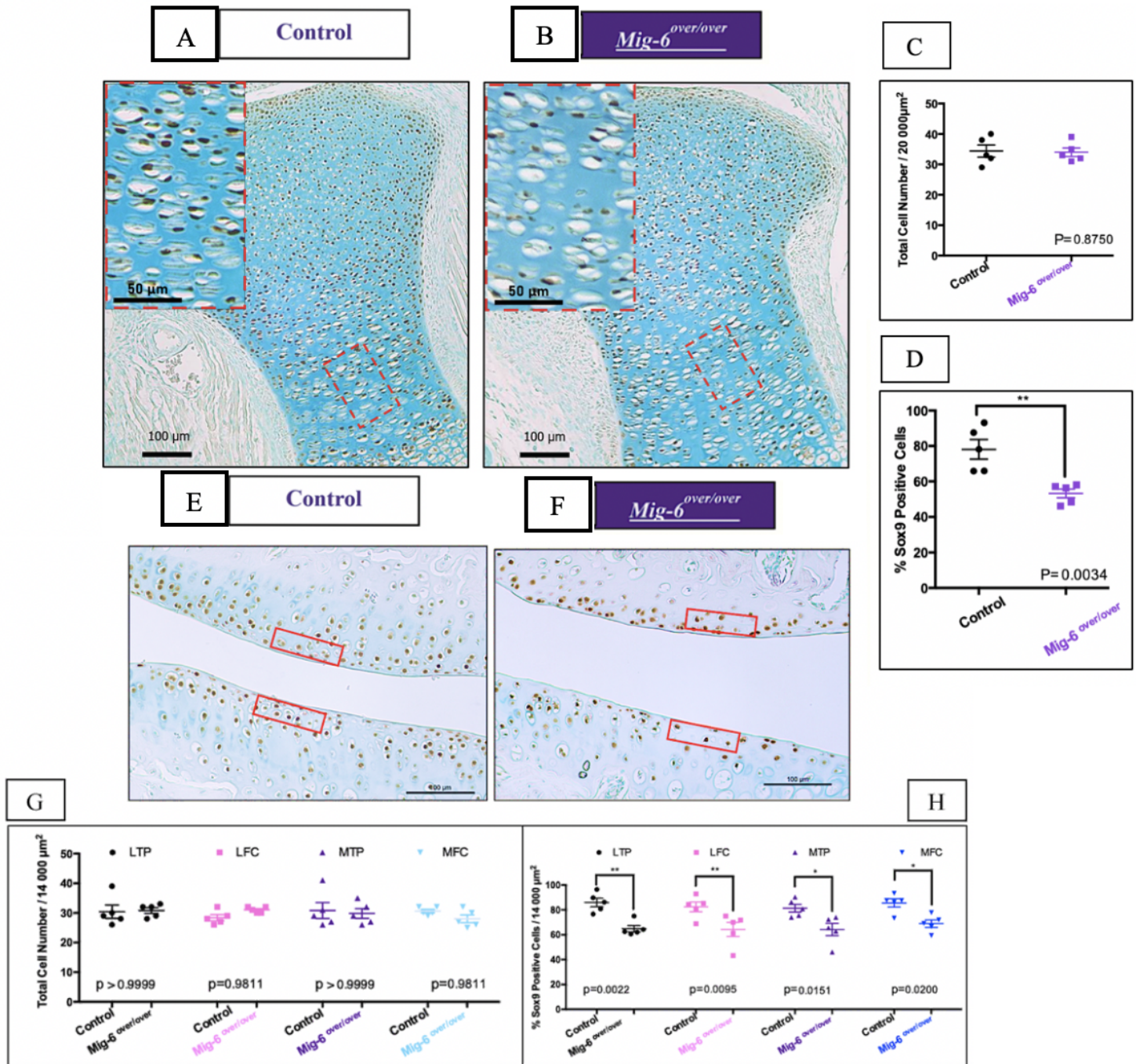


**Figure 5**

SOX9 immunostaining shows a decrease in positive cells in Mig-6 overexpressing mice at p0 and 6 weeks. Immunostaining of SOX9 in the knee joints of control (A/E) and Mig-6over/over (Mig-6over/overCol2a1-Cre+/-) (B/F) mice. Total cell number/area from control and Mig-6over/over mice (C/G). Percentage of Sox9 positive cells from control and Mig-6over/over at p0 and 6 weeks (D/H). Data

analyzed by two tailed student t-tests from 5 mice per group. Individual data points presented with mean  $\pm$  SEM ( $P < 0.05$ ). Scale bar = 100 $\mu$ m and 50 $\mu$ m.



## Figure 6

Lubricin immunostaining is slightly decreased in the articular cartilage of cartilage-specific Mig-6 overexpressing mice at 11 weeks of age. Immunostaining of sections of the knee joint indicate the presence of Lubricin (PRG4) in superficial zone chondrocytes. IHC reveals no staining for the negative control (C). Sections from Mig-6 KO mice served as positive control (D). N=4-5 mice/genotyping. Scale bar = 100 $\mu$ m.

## Supplementary Files

This is a list of supplementary files associated with this preprint. Click to download.

- [SupplementaryFigures.pdf](#)